ADVANCED OPTICAL MATERIALS
www.advopticalmat.de

Hybrid Perovskite Thin Films as Highly Efficient Luminescent Solar Concentrators

*Katerina Nikolaidou, Som Sarang, Christine Hoffman, Benaz Mendewala, Hidetaka Ishihara, Jennifer Q. Lu, Boaz Ilan, Vincent Tung, and Sayantani Ghosh**

Organic–inorganic hybrid perovskite (PVSK) compounds are at the forefront of photovoltaic research, consistently surpassing silicon solar cells in power conversion efficiency. Possessing high refractive index, broad absorption spectrum, and superior quantum yields, hybrid PVSK thin films are theoretically also ideal candidates for luminescent solar concentrators (LSCs). In practice, however, the possibility of high self-absorption in a continuous film, coupled with the inherent instability of PVSK materials, have hindered their use in this context. In this work, the viability of hybrid PVSK thin films as the active medium in planar LSCs is investigated. Using spectroscopic and photovoltaic measurements, variation of optical stability and device performance with different lead sources in the PVSK film precursors are monitored. The results display high optical efficiency in the range 15%–29% despite high self-absorption losses, and the devices remain operational even after seven weeks in ambient conditions. Confirmed by Monte Carlo simulations, the superior performance is attributed to the high quantum yield and refractive index of the PVSKs. These results are encouraging not only for the implementation of PVSK thin films in LSCs, but additionally, for preparation of tandem devices to capture energy escaping as radiative exciton recombination in PVSK solar cells.

1. Introduction

Luminescent solar concentrators (LSCs), proposed as alternatives to solar cells in the 1970s, typically consist of high refractive index substrates doped with photoluminescent materials that absorb both direct and diffuse sunlight. The resultant down-converted emission is then conveyed to the edges of the device by total internal reflection, to be captured by attached solar cells.[1–3] As the lateral surface area of an LSC is considerably larger than its edge area, the photon density incident on the solar cells is increased, named the "concentrator" effect. Additionally, by a propitious choice of the dopants, the emission can be spectrally-matched to the solar cell bandgap, further optimizing the generated photocurrent.[4] The initial motivation for LSCs had been financial, as large panels of glass or polymer materials were far less expensive than an equivalent sized solar panel.[5] With time, this aspect has been considerably negated, but LSCs remain of interest on account of other advantages they offer over conventional photovoltaics. One of these is the simplicity of fabrication compared to the multistep, and often rigorous, procedures involved in solar cell development. Other benefits include operation under both diffuse and direct lighting, which make tracking machinery and focusing optics unnecessary, and allow for mounting on vertical surfaces, greatly enhancing the deployable area, particularly in crowded urban landscapes.[1,5,6]

The characteristics of a desirable LSC candidate include high quantum yield (QY), large Stokes shift to minimize self-absorption, and broad spectral absorption range to collect as much sunlight as possible. The earliest materials used in LSCs were fluorescent organic dyes, followed by laser dyes,[1] both chosen for their high QYs. Optical efficiency of 40% has been achieved using a mixture of Lumogen F Red 305 dye in polymer, and power conversion efficiency of 7.1% has been reported using a combination of dyes with GaAs solar cells attached at the edges.[7,8] Higher power conversion efficiency of 14.5% has been achieved using a tandem planar solar concentrator, employing a mixture of dyes in combination with copper indium gallium selenide cells.[9] Dyes have inherent problems that include rapid photobleaching and narrow absorption bands,[10–12] and while there are some, such as Red305 by BASF that demonstrate long lifetimes and broad absorption spectra,[13,14] these are the exception rather than the rule. Consequently, the efforts to develop stable and high performing LSC active materials shifted to semiconducting quantum dots (QDs). QDs have broadband absorption extending from the band edge into the ultraviolet, and although the most commonly used QDs emit in the visible region,[15] there have been LSCs developed using QDs with narrow bandgaps emitting in the near infrared that are better spectrally-matched to silicon.[4]

K. Nikolaidou, S. Sarang, C. Hoffman, B. Mendewala, Prof. B. Ilan, Prof. S. Ghosh
School of Natural Sciences
University of California
Merced, CA 95344, USA
E-mail: sghosh@ucmerced.edu
Dr. H. Ishihara, Prof. J. Q. Lu, Prof. V. Tung
School of Engineering
University of California
Merced, CA 95344, USA

DOI: 10.1002/adom.201600634

"Giant" QDs designed to eliminate "blinking" and photo-degradation have emerged as yet another possible LSC candidate.[16] A recent development incorporating nontoxic QDs with high QY and a 150 nm Stokes shift has achieved optical efficiency of 26.5%, bringing LSCs one step closer to utilization in large area building integrated applications.[17–19] In addition to progress on the materials engineering front, there have been research efforts on modifying the standard planar architecture with other geometries, such as cylinders, where reduced self-absorption and increased scattering have enhanced device efficiency.[20]

Despite the progress outlined above, LSCs have not replaced traditional solar cells. While QD-based LSCs are an improvement over their dye-based counterparts, they also oxidize and degrade with time,[18,21] which is particularly severe for the near infrared emitting QDs. Additionally, most have low QY and have not demonstrated power conversion efficiencies above 9%.[1,4,9,22] In this paper, we move away from discrete fluorescent dopants, and examine the viability of continuous thin films of organic–inorganic hybrid perovskite (PVSK) as the active medium in planar LSCs. Hybrid PVSKs have dominated the photovoltaic field in the past few years as solution-processed high efficiency solar cells,[23] combining the ease of fabrication of organic materials with the high carrier mobility of inorganic semiconductors.[24] Typically, opaque thin films would not be ideal for LSCs due to high self-absorption, but PVSK materials have several advantages that could compensate for this aspect. These include an absorption band that spans a large portion of the solar spectrum, a high QY often reaching 80%[24,25] and a refractive index of 2.5, significantly larger than glass and polymer films, indicating the likelihood of more efficient confinement.[26,27] In a prior instance, PVSK films were used to coat a silicon solar cell to exploit the superior absorption and QY to improve the solar cell performance.[28] In our case, hybrid PVSK thin films are used in the traditional LSC configuration with silicon PV cells attached at the edges, and we focus on two main aspects in our study. The first is optimizing LSC performance with PVSK composition and film quality, achieved by varying the ratio of precursors during the synthesis stage. The second is investigating an issue that is a big hurdle to the deployment of PVSK photovoltaics in the field—the structural instability that causes rapid deterioration of film quality and electronic transport properties when exposed to humidity.[29,30] Our results reveal high optical efficiency (15%–29%), which we find to be strongly dependent on the sample preparation process, and we correlate device performance to optical quality by spatially-resolved photoluminescence (PL) spectroscopy, and to structural integrity via scanning electron microscopy (SEM). Additionally, our LSCs remain operational after seven weeks under ambient conditions, far longer than expected for a hybrid PVSK sample.

2. Results

2.1. Spectral and Morphological Characterization

Figure 1 summarizes the spectral properties of a characteristic PVSK thin film with 50% $PbAc_2$ content. The emission is centered at 780 nm with a full width at half maxima (FWHM) of

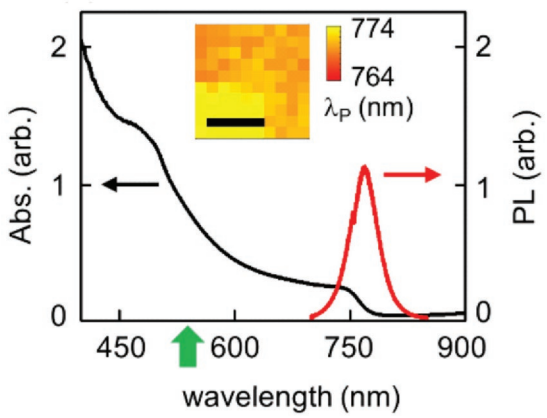

Figure 1. Absorption and PL emission spectra of PVSK thin film. Bold arrow shows laser excitation wavelength. (Inset) Spatially-resolved peak emission wavelength λ_P map. Scale bar is 25 μm.

40 nm. The absorption, uncharacteristically for 3D systems, spans the entire visible spectrum and extending into the near infrared. In traditional dye or QD doped LSCs, quality of surface emission is not an important indicator of device performance; edge emission is the critical parameter. For thin film PVSKs fabricated by solution-based processing techniques, however, surface emission uniformity is a reflection of sample crystallinity and structural homogeneity, and has become a necessary measurement for characterizing film quality[31,32] on a length scale larger than what is possible using electron microscopy. Spatial uniformity of spectral intensity and wavelength should reflect the lack of defects that serve as nonradiative recombination centers, which in turn could hinder LSC photocurrent output.[33,34] In the inset we plot the peak wavelength λ_P of a spatially resolved PL scan over a 50 μm^2 area. The variation is ≈10 nm, well within the FWHM of the emission, and signifies that our samples are spectrally homogenous and associated self-absorption losses will be as well. The use of $PbAc_2$ precursor has been previously shown to form highly uniform PVSK thin films due to the volatile nature of the by-product, whereas the longer annealing time required for $PbCl_2$ based PVSKs, which may produce larger crystals favorable for charge carrier transport, are prone to pore formation prior to crystallization.[35] In **Figure 2** we systematically correlate the stoichiometric ratio between Pb precursors and the corresponding optical quality and morphology of the thin films. As shown in the SEM images of the PVSK films in Figure 2a–d, films with 100% $PbAc_2$ are characterized by lack of pinholes and ultrasmooth surface, while increasing stoichiometric ratio of $PbCl_2$ leads to the formation of larger grains and abundant pinholes. The high density of pinholes has been associated with increased nonradiative recombination. The accompanying PL intensity maps show an interesting correlation between structural and optical qualities: the smooth 100% $PbAc_2$ film has PL emission that is expectedly very uniform, but of low intensity; the films with 95% and 90% acetate content have brighter but highly inhomogeneous PL; the 50% $PbAc_2$ sample appears to have the most homogenous PL emission that is also of high intensity. Based on these observations, an LSC with either 50% or 100% $PbAc_2$ would appear to have potential for most

Adv. Optical Mater. 2016,
DOI: 10.1002/adom.201600634

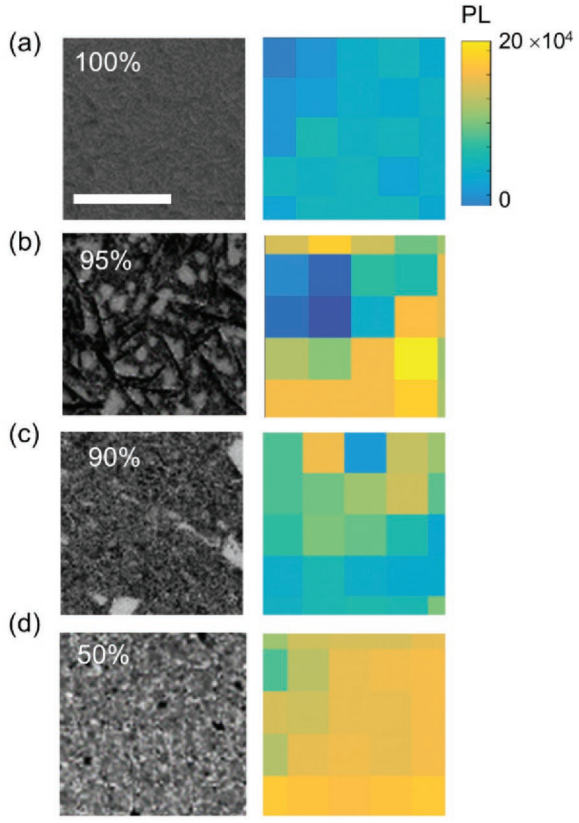

Figure 2. SEM images of samples with varying $PbAc_2$ content, along with spatially-resolved PL maps. a–d) 100%, 95%, 90%, and 50% acetate content, respectively. All images are 25 μm^2.

success. We additionally demonstrate (Figure S1, Supporting Information) that the 50% $PbAc_2$ sample has the highest external quantum efficiency (EQE), which is expected given that higher Cl content improves electronic properties.

2.2. Estimating Self-Absorption and Surface Losses

In addition to structural integrity and optical homogeneity, LSC active materials should aim to minimize self-absorption (SA) losses that arise from reabsorption of the light emitted by the active material itself along the optical path to the edges. SA is accompanied by a red-shift in emission wavelength as the more energetic photons are reabsorbed and subsequently re-emitted at lower energy (longer wavelength). To quantify SA, we use PL measurements in **Figure 3** with excitation and collection spatially separated by a distance d. The excitation spot is ≈1 µm, and the emission is collected using a fiber optic at the edge of the device. Figure 3a,b summarize the results obtained using 532 nm laser excitation and shows PL intensity and peak wavelength red-shift ($\Delta\lambda_P$) as a function of d, data taken four weeks apart. The maximum value of d is 12 mm, limited by the size of the samples. PL intensity taken as soon as the samples are prepared decreases by 90% with increasing d but $\Delta\lambda_P$ only shifts by 3 nm over the same length. Such small red-shift is indicative of minor SA by the PVSK film, which implies the accompanying

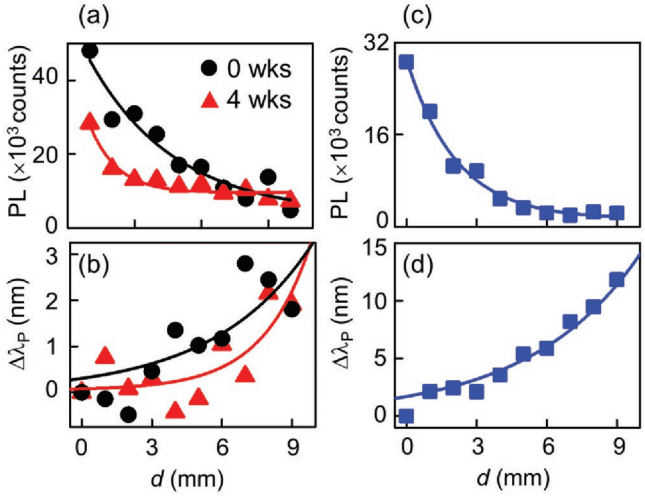

Figure 3. a) PL and b) peak wavelength shift $\Delta\lambda_P$ varying with pump-probe separation d measured using laser excitation. c) PL and d) $\Delta\lambda_P$ measured with broadband white light excitation.

intensity drop is most likely due to top/bottom surface losses. Data re-taken after the samples are exposed to ambient conditions for four weeks do not show significant change in $\Delta\lambda_P$, and PL intensity now drops by 75%. This is an encouraging result as it indicates that despite the instability of PVSK in photovoltaic applications, the optical properties are far more stable and will thus enable more viable alternative applications. To gain a more realistic picture of the SA losses, we repeat the measurements with a broadband white light source in Figure 3c,d. In this case, PL intensity decreases more rapidly than in Figure 3a, and $\Delta\lambda_P$ is much larger, measuring 15 nm over the same range of d. Large SA is expected in a continuous film, but it is significant that SA is higher with white light in comparison to illumination by monochromatic light. This may be attributed to the differential absorption of PVSKs over the spectral range of the broadband source, which results in the production of fewer photo-generated carriers on average compared to excitation by 532 nm.[36,37]

To accurately estimate both SA and surface losses that would be associated with our samples when exposed to the solar spectrum, we perform 3D Monte Carlo simulations for three different types of LSCs, which include (i) thin film PVSK with refractive index 2.5, and QY = 0.8, (ii) PVSK QDs embedded in a substrate with refractive index 1.7, and QY = 0.8, and (iii) CdSe/CdTe core-shell QDs embedded in a substrate with refractive index 1.7, and QY = 0.9. The substrate refractive index used is 1.7 instead of the more common 1.5 to mimic our indium tin oxide (ITO) coated glass substrates. We note here however, that we have repeated simulations of (ii) and (iii) with a refractive index of 1.5 and the results are practically unchanged. CdSe/CdTe QDs typify dots emitting in the visible spectrum used in LSCs. We include PVSK QDs in our calculations as they share the high QY of their thin film counterparts and may have lower SA. **Figure 4** summarizes the results. Figure 4a shows histograms representing the number of absorption events that each photon undergoes in all three materials. Ideally, each photon should undergo a single absorption event and then be re-emitted to propagate up to the edges. If

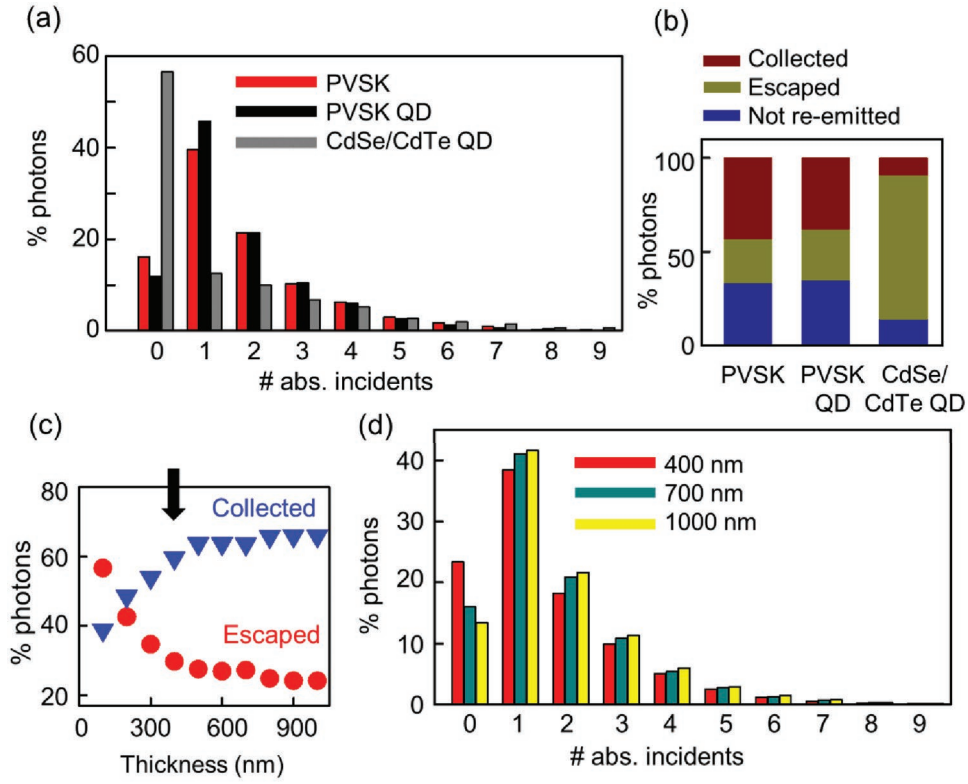

Figure 4. a) Calculated distribution of reabsorption events of absorbed photons for different LSC materials. b) Relative proportions of photons collected, escaped and not re-emitted. c) Photon collection and escape percentages varying with PVSK thin film thickness. Arrow indicates thickness of thin films used in the experiment. Note: these are deposited on a 1 mm glass substrate. d) Absorption events varying with PVSK film thickness.

that were the case, the second column from the left (labeled "1") would have 100% of the photon counts. In the thin film PVSK sample more than 40% of the incident photons undergo a single absorption and re-emission event, with less than 20% of the incident photons not being absorbed at all, and even fewer undergoing multiple absorption (self-absorption) events, attesting to efficient absorption and adequate Stokes shift. The histogram using the PVSK QDs is comparable to the thin film. In contrast, the CdSe/CdTe QDs results in most of the photons (> 50%) not being absorbed at all, and only 15% being absorbed exactly once, which is quite wasteful. In Figure 4b we compile the proportions of photons that are lost through the surfaces, that are not re-emitted, and that are ultimately collected. For the two LSCs based on PVSK, ≈40% of the incident photons are collected, compared to only 9% in CdSe/CdTe LSCs. To obtain a meaningful comparison, the optimal QD concentrations for maximal optical gain were used, which corresponds to volume fractions of 10^{-4} and 10^{-3} for the PVSK and CdSe/CdTe QDs, respectively. Even though the PVSK QY was below that of CdSe/CdTe QDs, the results using the PVSK QDs are better because its larger Stokes shift allows for a tenfold higher concentration. In all these simulations we have assumed a mirror coated bottom surface and silicon PV cells on all four sides. The PVSK simulations used the experimental absorption and PL data reported here and the CdSe/CdTe simulations used measured optical properties in prior work.[38] The sunlight is incident normal to the surface and its spectrum is sampled from the solar irradiance.[39] Further details on the Monte Carlo method used can be found in refs. [38,40]. We calculate the amount of collected and escaped photons as a function of PVSK film thickness in Figure 4c. For the thickness of our samples, ≈400 nm, 60% of the incident photons are collected. Higher thickness, as these results indicate, could improve light absorption. However, Figure 4d shows that while increased film thickness does lead to better absorption, with the highest percent of single absorption events, it also has higher proportion of subsequent absorption counts. This implies increased thickness is also associated with greater self-absorption, thereby negating the initial benefit of enhanced light absorption.

2.3. Optical Efficiency and Device Stability

In **Figure 5** we monitor the effect of the ratio of $PbAc_2$ to $PbCl_2$ in the PVSK precursor solution on absorption, SA, and LSC-to-PV current ratio. As shown in Figure 5a, SA, directly proportional to the measured spectral red-shift $\Delta\lambda_p$, increases almost monotonically with acetate content, while absorption, shown in Figure 5b, starts increasing around $PbAc_2$ content of 80%, peaking at 98%. Figure 5c shows the current generated by each of these. In the low $PbAc_2$ regime (50% acetate), as the uniform PL scan in Figure 2d indicated, SA is low, but unfortunately so is the total absorption, resulting in low total I_{LSC}. With 100% acetate, PL scan in Figure 2a had been homogenous but of low intensity, and here it exhibits high SA cancelling the

Adv. Optical Mater. 2016,
DOI: 10.1002/adom.201600634

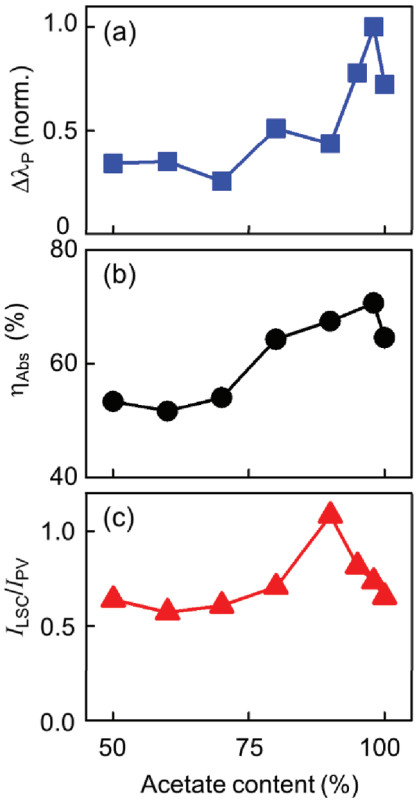

Figure 5. a) $\Delta\lambda_P$, b) η_{Abs}, and c) current ratio I_{LSC}/I_{PV} varying with $PbAc_2$ content.

advantage of high absorptance. The highest current is observed in the PVSK sample with 90% $PbAc_2$ and these results indicate the SEM images and PL scans do not accurately predict photocurrent generation ability, and neither does EQE data. As with other LSC materials the ratio of absorption to SA is the most critical factor. Using the current I_{LSC} we can calculate the optical efficiency using $\eta_{opt} = \frac{I_{LSC} \times A_{PV}}{I_{PV} \times A_{LSC}}$.[5] The concentration factor is defined as the ratio of the areas of the LSC and the PV cells attached at the edges and taking the entire circumference into account, it is 3.75 for our samples, resulting in the optical efficiency shown in **Figure 6**. Expectedly, η_{opt} follows the same trend with $PbAc_2$ as the I_{LSC} data in Figure 5c, exhibiting a maximum of 29% for PVSK film with 90% acetate content.

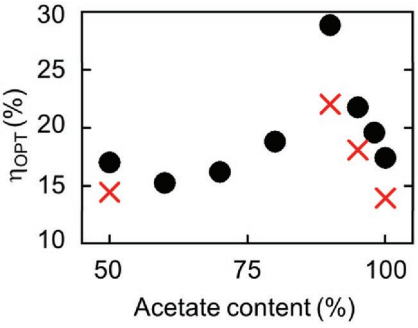

Figure 6. Optical efficiency η_{OPT} varying with $PbAc_2$ content immediately after PVSK film synthesis (circles) and after four weeks (crosses).

This is an impressive result, one of the highest optical efficiencies reported in semiconductor-based LSCs, demonstrating the suitability of PVSK films as LSC active material. Even the worst device has an efficiency of 15%. Finally, given the concern regarding the stability of hybrid PVSKs, we follow up with photocurrent measurements after four weeks. The optical efficiency and current output is surprisingly stable, dropping by 15%–20% across the different devices, shown in Figure 6. We continued monitoring performance up to seven weeks, by which time I_{LSC} decreases by a further 5%. Such long device stability is unusual for PVSK based devices due to degradation of the PVSK thin film upon exposure to moisture. When certain regions of the PVSK thin film degrade, efficient electron transport is hindered and is thus detrimental to electrical properties of the entire film. However, the film still emits efficiently and since LSCs are purely optical devices, they can be operational in this case. Furthermore, the degradation of PVSK thin film regions results in reduced self-absorption as shown in Figure 3, where I_{PL} drops by a smaller amount in the four-week old sample, thus allowing for fewer losses in the older devices and ultimately compensating for the lower initial emission. The power conversion efficiency of the devices is estimated to vary between 7% and 13%, and follows the same trend as optical efficiency, calculated using the fill factor from the standard current–voltage curve of a PV cell (Figure S2, Supporting Information).

3. Conclusion

PVSK films perform very well as active media in LSCs, borne out here by the experimental results and confirmed by simulations. Devices with optical efficiency reaching 29% have been fabricated, with the lowest optical efficiency being 15%, whereas the devices were still operational seven weeks later. This superior photocurrent output is resultant of several positive attributes. These include high quantum yield combined with a large refractive index that confines most of the photons in the films. Furthermore, the 780 nm centered emission achieves good spectral matching with the absorption of silicon PV cells, allowing the latter to perform under optimal external quantum efficiency conditions. Tapping into the inherent property of fluorescent materials to down-convert the incident solar light to a more favorable wavelength[22] for solar cells is a central tenet of LSCs. This is the reason that for use with silicon PVs, LSC fluorophores emitting in the far red or near infrared have been so sought after.[41] Dyes are rare at this part of the spectrum and QDs such as PbSe and PbS have low QY and poor photo stability. Hybrid perovskites address most of these concerns and as our time-delayed studies confirm, even though $PbAc_2$ based PVSK thin films are usually associated with quick degradation, their optical properties are preserved for longer, opening a new realm of possibilities for PVSK-based optical devices.[24,42] This study further provides useful insights for optimizing future endeavors of implementing PVSK LSCs. Based on our present results, PVSK LSCs will require significant device engineering before achieving commercialization. Despite the longevity of these devices when compared to PVSK solar cells, efforts to extend their lifetime further is necessary. Such efforts could

include encapsulation of films between transparent metal oxides, previously shown to prolong device lifetime in photovoltaic devices.[43] In addition, bottom surface losses could be minimized by deployment of substrates with higher refractive index than glass. PVSK films in photovoltaic device are adjacent to a metal oxide or polymer layer, which commonly have refractive indices higher than glass,[44] and as these deposition techniques have been optimized already, adopting these protocols for LSC devices will prove simple and low cost alternatives.[45,46] Lastly, self-absorption may be reduced by using PVSK quantum dots and spectral filtering of incident radiation, as it has been demonstrated (Figure 3) that selective illumination of PVSK LSCs with a single wavelength reduces the observed emission red-shift and subsequently, self-absorption. Both modifications would aid greatly toward enhancing optical efficiency.

4. Experimental Section

PVSK precursor solutions of different lead sources are prepared using as-synthesized methylammonium iodide (MAI) (Luminescence Technology Corp.) and various ratios of lead (II) acetate trihydrate ($PbAc_2$, Sigma Aldrich) to lead (II) chloride ($PbCl_2$, Sigma Aldrich); the ratios used are 1:1, 9:1, 19:1, 49:1, and 1:0. For PVSK precursor solutions based on $PbAc_2$ or PbI_2, the only halide present is I, which results in the production of methylammonium lead triiodide ($CH_3NH_3PbI_3$) films. On the other hand, PVSK prepared from precursor solution with $PbCl_2$ contains both I and Cl, thus forming a mixed halide PVSK ($CH_3NH_3PbI_{3-x}Cl_x$).[35] The precursors are dispersed in a bisolvent system of anhydrous dimethyl sulfoxide and *N*-methyl-2-pyrrolidione (4:6, v/v) in concentrations of 2.64 M for MAI and 0.88 M for the lead source, respectively.[31,32] PVSK thin films are prepared on UV-ozone treated ITO substrates by spin coating in a nitrogen environment at 4000 rpm for 30 s and are subsequently annealed in a vacuum oven at 60 °C for 20 min. The absorbance spectra are obtained using an Agilent UV–vis spectrophotometer. The PL measurements are done using a 532 nm continuous wave diode laser (Verdi V6, Coherent Inc.) and the spectra are recorded using a 300 mm Acton spectrometer with a thermoelectrically cooled charge-coupled device (spectral resolution ≈0.18 nm). White light experiments are conducted using a broadband source (Motic MLC—150C). SEM images are acquired using Zeiss Gemini SEM 500. Photocurrent measurements are done using a calibrated silicon PV of active area 15×1 mm^2 attached to the edge of the LSC of size $15 \times 15 \times 1$ mm^3 and are conducted outdoors to leverage the solar spectrum.

Supporting Information

Supporting Information is available from the Wiley Online Library or from the author.

Acknowledgements

This research was supported by funds from the National Aeronautics and Space Administration (NASA) grant no. NNX15AQ01A. V.T. gratefully acknowledges the support of user proposals (#3192 and #3715) at the Molecular Foundry, Lawrence Berkeley National Lab, supported by the Office of Basic Energy Sciences, of the U.S. Department of Energy under grant No. DE-AC02-05CH11231.

Received: August 1, 2016
Revised: August 28, 2016
Published online:

[1] M. G. Debije, P. P. C. Verbunt, *Adv. Energy Mater.* **2012**, *2*, 12.
[2] W. H. Weber, J. Lambe, *Appl. Opt.* **1976**, *15*, 2299.
[3] A. Goetzberger, W. Greubel, *Appl. Phys.* **1977**, *14*, 123.
[4] G. V. Shcherbatyuk, R. H. Inman, C. Wang, R. Winston, S. Ghosh, *Appl. Phys. Lett.* **2010**, *16*, 191901.
[5] V. Sholin, J. D. Olson, S. A. Carter, *J. Appl. Phys.* **2007**, *101*, 123114
[6] M. G. Debije, V. A. Rajkumar, *Sol. Energy* **2015**, *122*, 334.
[7] G. D. Gutierrez, I. Coropceanu, M. G. Bawendi, T. M. Swager, *Adv. Mater.* **2016**, *28*, 497.
[8] L. H. Slooff, E. E. Bende, A. R. Burgers, T. Budel, M. Pravettoni, R. P. Kenny, E. D. Dunlop, A. Büchtemann, *Phys. Stat. Sol. RRL* **2008**, *2*, 257.
[9] M. J. Currie, J. K. Mapel, T. D. Heidel, S. Goffri, M. A. Baldo, *Science* **2008**, *321*, 226.
[10] W. G. J. H. M. van Sark, K. W. J. Barnham, L. H. Slooff, A. J. Chatten, A. Büchtemann, A. Meyer, S. J. McCormack, R. Koole, D. J. Farrell, R. Bose, E. E. Bende, A. R. Burgers, T. Budel, J. Quilitz, M. Kennedy, T. Meyer, C. De Mello Doneg, A. Meijerink, D. Vanmaekelbergh, *Opt. Express* **2008**, *16*, 21773.
[11] L. H. Slooff, N. J. Bakker, P. M. Sommeling, A. Büchtemann, A. Wedel, W. G. J. H. M. van Sark, *Phys. Stat. Sol. A* **2014**, *211*, 1150.
[12] G. Griffini, L. Brambilla, M. Levi, M. Del Zoppo, S. Turri, *Sol. Energy Mater. Sol. Cells* **2013**, *111*, 41.
[13] G. Seybold, G. Wagenblast, *Dyes Pigm.* **2009**, *11*, 303.
[14] M. G. Debije, P. P. C. Verbunt, P. J. Nadkarni, S. Velate, K. Bhaumik, S. Nedumbamana, B. C. Rowan, B. S. Richards, T. L. Hoeks, *Appl. Opt.* **2011**, *50*, 163.
[15] I. Coropceanu, M. G. Bawendi, *Nano Lett.* **2014**, *14*, 4097.
[16] F. Meinardi, A. Colombo, K. A. Velizhanin, R. Simonutti, M. Lorenzon, L. Beverina, R. Viswanatha, V. I. Klimov, S. Brovelli. *Nat. Photonics* **2014**, *8*, 392.
[17] L. R. Bradshaw, K. E. Knowles, S. McDowall, D. R. Gamelin, *Nano Lett.* **2015**, *15*, 1315.
[18] F. Meinardi, H. McDaniel, F. Carulli, A. Colombo, K. A. Velizhanin, N. S. Makarov, R. Simonutti, V. I. Klimov, S. Brovelli, *Nat. Nanotechnol.* **2015**, *10*, 878.
[19] C. Li, W. Chen, D. Wu, D. Quan, Z. Zhou, J. Hao, J. Qin, Y. Li, Z. He, K. Wang, *Sci. Rep.* **2015**, *5*, 17777.
[20] R. H. Inman, G. V. Shcherbatyuk, D. Medvedko, A. Gopinathan, S. Ghosh, *Opt. Express* **2011**, *19*, 24308.
[21] S. R. Cordero, P. J. Carson, R. A. Estabrook, G. F. Strouse, S. K. Buratto, *J. Phys. Chem. B* **2000**, *104*, 12137.
[22] Y. Zhou, D. Benetti, Z. Fan, H. Zhao, D. Ma, A. O. Govorov, A. Vomiero, F. Rosei, *Adv. Energy Mater.* **2016**, *6*, 1501913.
[23] W. Nie, H. Tsai, R. Asadpour, J. C. Blancon, A. J. Neukirch, G. Gupta, J. J. Crochet, M. Chhowalla, S. Tretiak, M. A. Alam, H. L. Wang, A. D. Mohite, *Science* **2015**, *347*, 522.
[24] T. Leijtens, G. E. Eperon, N. K. Noel, S. N. Habisreutinger, A. Petrozza, H. J. Snaith, *Adv. Energy Mater.* **2015**, *5*, 1500963.
[25] M. Saba, M. Cadelano, D. Marongiu, F. Chen, V. Sarritzu, N. Sestu, C. Figus, M. Aresti, R. Piras, A. Geddo Lehmann, C. Cannas, A. Musinu, F. Quochi, A. Mura, G. Bongiovanni, *Nat. Commun.* **2014**, *5*, 5049.
[26] P. Löper, M. Stuckelberger, B. Niesen, J. Werner, M. Filipič, S. J. Moon, J. H. Yum, M. Topič, S. De Wolf, C. Ballif, *J. Phys. Chem. Lett.* **2015**, *6*, 66.
[27] C. W. Chen, S. Y. Hsiao, C. Y. Chen, H. W. Kang, Z. Y. Huang, H. W. Lin, *J. Mater. Chem. A* **2015**, *3*, 9152.
[28] S. Mirershadi, S. Ahmadi - Kandjani, *Dyes Pigm.* **2015**, *120*, 15.
[29] J. Yang, B. D. Siempelkamp, D. Liu, T. L. Kelly, *ACS Nano* **2015**, *9*, 1955.
[30] J. A. Christians, P. A. Miranda Herrera, P. V. Kamat, *J. Am. Chem. Soc.* **2015**, *137*, 1530.
[31] H. Ishihara, S. Sarang, Y. C. Chen, O. Lin, P. Phummirat, L. Thung, J. Hernandez, S. Ghosh, V. Tung, *J. Mater. Chem. A* **2016**, *4*, 6989.

[32] H. Ishihara, W. Chen, Y. C. Chen, S. Sarang, N. De Marco, O. Lin, S. Ghosh, V. Tung, *Adv. Mater. Interfaces* **2016**, *3*, 1500762.
[33] H. S. Duan, H. Zhou, Q. Chen, P. Sun, S. Luo, T. B. Song, B. Bob, Y. Yang, *Phys. Chem. Chem. Phys.* **2015**, *17*, 112.
[34] W. Qiu, T. Merckx, M. Jaysankar, C. Masse de la Huerta, L. Rakocevic, W. Zhang, U. W. Paetzold, R. Gehlhaar, L. Froyen, J. Poortmans, D. Cheyns, H. J. Snaith, P. Heremans, *Energy Environ. Sci.* **2016**, *9*, 484.
[35] W. Zhang, M. Saliba, D. T. Moore, S. K. Pathak, M. T. Hörantner, T. Stergiopoulos, S. D. Stranks, G. E. Eperon, J. A. Alexander-Webber, A. Abate, A. Sadhanala, S. Yao, Y. Chen, R. H. Friend, L. A. Estroff, U. Wiesner, H. J. Snaith, *Nat. Commun.* **2015**, *6*, 6142.
[36] C. Wehrenfennig, M. Liu, H. J. Snaith, M. B. Johnston, L. M. Herz, *APL Mater.* **2014**, *2*, 081513.
[37] J. F. Galisteo-López, M. Anaya, M. E. Calvo, H. Míguez, *J. Phys. Chem. Lett.* **2015**, *6*, 2200.
[38] D. Şahin, B. Ilan, D. F. Kelley, *J. Appl. Phys.* **2011**, *110*, 033108.
[39] K. Emery, Tech. Rep., ASTM. **2000**, http://rredc.nrel.gov/solar/spectra/am1.5.
[40] D. Şahin, B. Ilan, *J. Opt. Soc. A* **2013**, *30*, 813.
[41] H. Field, in *IEEE Photovoltaic Specialists Conf.*, IEEE, Piscataway, NJ, USA **1997**, p. 471.
[42] F. K. Aldibaja, L. Badia, E. Mas-Marzá, R. S. Sánchez, E. M. Barea, I. Mora-Sero, *J. Mater. Chem. A* **2015**, *3*, 9194.
[43] J. You, L. Meng, T. Song, T. Guo, Y. Yang, W. Chang, Z. Hong, H. Chen, H. Zhou, Q. Chen, Y. Liu, N. De Marco, Y. Yang, *Nat. Nanotechnol.* **2016**, *11*, 75.
[44] S. Y. Kim, *Appl. Opt.* **1996**, *35*, 6703.
[45] J. Y. Kim, S. H. Kim, H. Lee, K. Lee, W. Ma, X. Gong, A. J. Heeger, *Adv. Mater.* **2006**, *18*, 572.
[46] D. Liu, T. L. Kelly, *Nat. Photonics* **2014**, *8*, 133.